Available online at www.sciencedirect.com
ScienceDirect
Journal of the European Ceramic Society 26 (2006) 3903–3908
www.elsevier.com/locate/jeurceramsoc

SiCN/C-ceramic composite as anode material for lithium ion batteries

Robert Kolb, Claudia Fasel, Verena Liebau-Kunzmann, Ralf Riedel *

Darmstadt University of Technology, Institute of Materials Science, Petersenstr. 23, D-64287 Darmstadt, Germany

Received 8 October 2005; received in revised form 22 December 2005; accepted 6 January 2006
Available online 3 March 2006

Abstract

The choice of electrode and electrolyte materials to design lithium batteries is limited due to the chemical reactivity of the used materials during the intercalation/deintercalation process. Amorphous silicon carbonitride (SiCN) ceramics are known to be chemically stable in corrosive environments and exhibit disordered carbonaceous regions making it potentially suitable to protect graphite from exfoliation. The material studied in this work was synthesized by mixing commercial graphite powder with the crosslinked polysilazane VL20®. Pyrolysis of the polymer/graphite compound at appropriate temperatures in inert argon atmosphere resulted in the formation of an amorphous SiCN/graphite composite material. First electrochemical investigations of pure SiCN and of the SiCN/C composite are presented here. A reversible capacity of 474 mA hg^{-1} was achieved with a sample containing 25 wt% VL20® and 75 wt% graphite. The measured capacity exceeds that of the used graphite powder by a factor of 1.3 without any fading over 50 cycles.

Keywords: Precursors-organic; Mechanical properties; Glass; Poisson's ratio; SiCN/C; Batteries

1. Introduction

The expanding market of portable electronic devices results in an increasing interest in compact, light-weight rechargeable batteries offering high energy densities. Concerning these demands a huge progress was achieved with the development of systems based on lithium ions as charge carrier. Permanent improvements were realized by the development of new materials for electrodes and electrolytes.[1–3] With respect to the anode site of the battery, metallic lithium[4] was the only real alternative due to its high theoretical capacity (3862 mA hg^{-1}) for a long time. Unfavourable properties such as dendritic crystal growth during charge and discharge of the battery[5] and its sensitivity to oxidation had to be accepted. First in 1989 carbon based materials were applied[6,7] and established by Sony Energytech,[8] which are used in most of the commercial lithium ion battery systems up to now. Despite the advantages of carbon based anodes like low cost and easy handling, there are some disadvantages related to its reactivity during charging and discharging. The amount of reaction between electrolyte and graphite strongly depends on the composition of the electrolyte and of the morphology, surface area, particle size and shape of the graphite particles.[3] Additionally, the limitation in the theoretical capacity (372 mA hg^{-1}) requires the search for new or modified anode materials for lithium ion batteries. These materials should exhibit the following enhanced properties: (i) chemical resistance against the electrolyte; (ii) high capacity; (iii) minor volume change during charge and discharge; (iv) low cost and low weight as well as (v) high Li mobility to achieve high charge currents. Some actual trends concerning anode materials are presently focussed on lithium alloys,[9,10] nano-alloys,[11] amorphous silicon[12,13] and carbon coated silicon,[13–15] polymer derived carbonitrides[16–18] and silicon carbide (SiC)[19,20] as well as surface modified graphite.[21,22] Furthermore, the influence of the surface modification of graphite on the exfoliation is still under discussion.[3] The above mentioned reference works clearly indicate that there is still need for alternative anode materials.

In this paper we focus on the surface modification of commercial graphite, known to exhibit exfoliation, by amorphous silicon carbonitride (SiCN). The samples were derived from a powder mixture of poly(organosilazane) and graphite forming a SiCN/graphite composite after pyrolysis at $T > 1000\,^{\circ}C$. It is known that polymer derived SiCN forms disordered carbons

* Corresponding author. Tel.: +49 6151 166347; fax: +49 6151 166346.
E-mail address: riedel@materials.tu-darmstadt.de (R. Riedel).

0955-2219/$ – see front matter © 2006 Elsevier Ltd. All rights reserved.
doi:10.1016/j.jeurceramsoc.2006.01.009

depending on the applied pyrolysis conditions.[23] This disordered carbon is assumed to act as percolation path for lithium as well as for electrons. Moreover, the chemical stability of SiCN should inhibit graphite from exfoliation. Therefore, the novel composite material is expected to combine the chemical stability of amorphous and low dense SiCN ceramics with the high capacity of graphite. In general commercial anodes consist of a mixture of lithium storage agent, organic binder and conductive additive. In case that SiCN exhibits the assumed percolation path for electrons and lithium ions, it can combine binder phase and conductive additive in one material. To analyse this effect in this study the electrochemical behaviour of pure graphite without binder and conductive additive was compared to that of SiCN/graphite composite.

2. Experimental

Commercially available polysilazane VL20® (KiON Inc., USA, details concerning the toxicity of VL20® can be found in the materials safety data sheet; www.kioncorp.com) with the formal composition $[SiCH_3RNR']_n$ (R = H, CH_3, vinyl; R′ = H, alkyl) was used as precursor for the synthesis of amorphous silicon carbonitride, SiCN. The polysilazane was partially crosslinked at 230 °C for 3.5 h in inert argon atmosphere using the Schlenk technique. Subsequently it was ground by rotating in a glass bottle with Al_2O_3 balls. Homogenization of a mixture comprised of 25 wt% VL20® and 75 wt% graphite powder (Fluka, Germany, purum, grain size <100 μm) was carried out over night in a planetary ball mill at 180 rpm. Finally, the powder mixture was pyrolysed using BN crucibles in a GERO tube furnace in inert argon atmosphere between 450 and 1250 °C. In the following, these samples are denoted as 25VL20-75C. For comparison pure crosslinked VL20® was pyrolysed between 1150 and 1550 °C. Heating and cooling rates were set to 100 °C/h and the holding time at the final temperature was 1 h. X-ray diffraction measurements were carried out on a Stoe Stadi P powder diffractometer using Mo $K\alpha_1$ radiation (λ = 0.709 Å). Nitrogen and oxygen elemental analyses were carried out with a LECO TC-436 using hot gas extraction technique. The carbon content of pure SiCN was measured using combustion analsis by the C-Analyzer Leco C-200. Scanning electron microscopy (SEM) imaging was performed on a JEOL 3600F Microscope, which was operated with an accelerating voltage of 5 kV. The specific surface area of the samples has been determined using nitrogen adsorption measurements by a QUANTACHROM Autosorb-3B instrument. Prior to the measurement the samples were heated for 24 h at 200 °C under vacuum. For electrochemical investigations charge/discharge experiments were performed at a constant current of 0.1 mA in the potential range between 0 and 3.5 V versus Li/Li^+ conducted in an electrolyte containing 1 M $LiPF_6$ in 1:1 ethylene carbonate (EC):dimethyl carbonate (DMC). Metallic lithium was used as counter and reference electrode and stainless steel as current collector. The powdered samples were manually pressed and assembled in Swagelok cells and a glass micro-fibre was used as separator. All the work has been done in inert argon atmosphere.

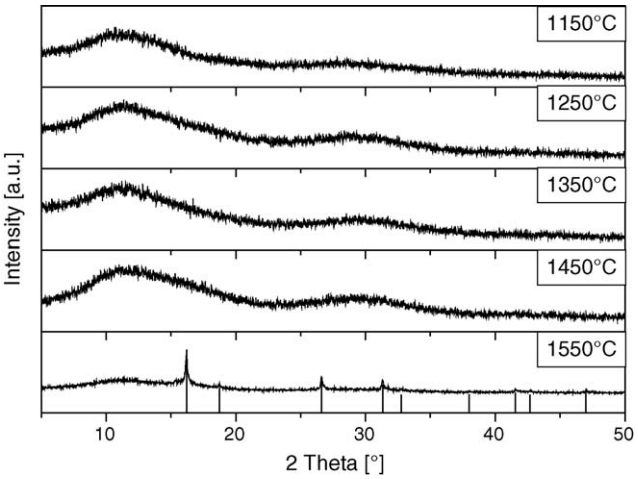

Fig. 1. X-ray diffraction pattern of pure SiCN derived from VL20® and pyrolysed at different temperatures, β-SiC phase is marked with bars.

3. Results and discussion

As shown in Fig. 1 pure polysilazane VL20® derived SiCN ceramics remain amorphous up to temperatures of 1450 °C. After heat treatment at 1550 °C silicon carbide is identified as crystalline phase, exclusively. This finding coincides with the work of Li et al.[24] who reported on the high temperature behaviour of SiCN synthesized from the related polysilazane CERASET™ (KiON Inc., USA).

The first charge/discharge and second charge cycles of pure VL20® pyrolysed at 1350 °C versus Li/Li^+ are shown in Fig. 2. Obviously Li intercalation starts at a potential exceeding 1 V versus Li/Li^+ as well as a hysteresis between charge and discharge is observed, which indicates the presence of disordered carbons.[3,25]

A distinction is drawn between disordered carbons formed at pyrolysis temperatures above 1000 °C, denoted as soft carbons, and disordered carbons formed at temperatures below 1000 °C, denoted as hard carbons. The main difference between both car-

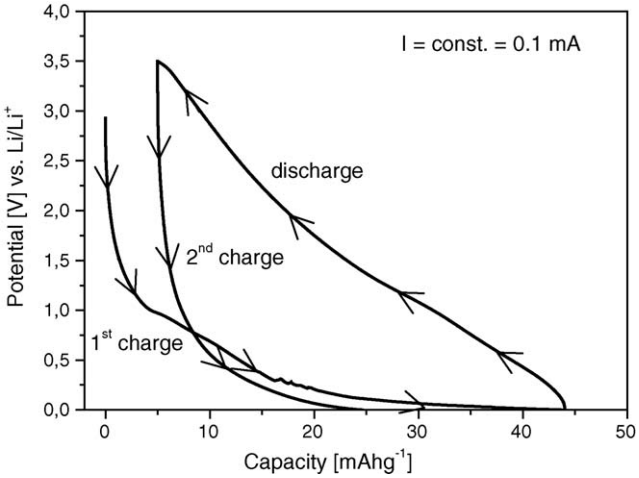

Fig. 2. First charge/discharge and second charge of VL20®/Li pyrolysed at 1350 °C.

Table 1
Capacity of the first charge (C_{charge}) and discharge ($C_{discharge}$) cycle vs. Li/Li$^+$, coulombic efficiency (η), carbon, nitrogen and oxygen content of pure SiCN derived from VL20® pyrolysed at different temperatures

T_{pyr} (°C)	C_{charge} (mA hg^{-1})	$C_{discharge}$ (mA hg^{-1})	η (%)	C (wt%)	N (wt%)	O (wt%)
1150	14	6	42.9	19.9	20.6	4.1
1250	10	7	70.0	19.9	20.9	4.7
1350	44	39	88.6	16.9	21.9	7.2
1450	27	11	40.7	17.9	21.7	1.3
1550	15	4	26.7	20.6	16.4	1.7

bons is the lower capacity of 150–200 mA hg^{-1} analysed for soft carbons and a higher capacity of 600–800 mA hg^{-1} for hard carbons. In our case the low capacities as well as the high pyrolysis temperatures above 1000 °C indicate the presence of soft carbons as part of the SiCN matrix.

The coulombic efficiency, defined as the ratio between two consecutive charge and discharge capacities, increases with the annealing temperature (Table 1).

At annealing temperatures exceeding 1350 °C the capacities as well as the coulombic efficiency drop down remarkably. Larcher et al. found a similar behaviour in pyrolysed pitch/polysilane mixtures.[26] They observed a loss of capacity with increasing amount of SiC phase, which was found to be inactive with respect to Li intercalation. The same effect is discussed in our case. As the SiC phase first appears at temperatures above 1450 °C and the capacity starts to decrease after annealing of the sample at 1350 °C, an additional aspect seems to be involved. The loss of capacity is discussed in terms of the chemical composition as shown in Table 1. A correlation between the oxygen content and the reversible capacity indicates a possible influence of oxygen on the electrochemical behaviour. In ref.[26] a similar relationship between the oxygen content and the capacity is discussed. In that particular work the amount of oxygen is directly correlated with the appearance of a SiC phase. As this interdependence is not found in our work, the significant loss of oxygen and the preceding change of the microstructure after heating at $T \geq 1450$ °C due to the beginning crystallization (see Fig. 1) have to be considered here.

Despite the fact that no detailed mechanism can be derived from our studies so far, our results clearly show that amorphous SiCN is suitable for intercalation/deintercalation of lithium. Therefore, the SiCN ceramic can be used to improve the chemical and mechanical resistance of electrode materials in lithium ion batteries. For this purpose a powder mixture containing graphite and partially crosslinked polysilazane VL20® was pyrolysed at different temperatures. Fig. 3 represents the observed diffraction patterns of the prepared samples. Beside graphite no additional crystalline phases could be identified up to a pyrolysis temperature of 1250 °C.

The cycling experiments as given in Fig. 4 clearly show that the capacity could be improved up to a factor of 1.3 for the 25VL20-75C-sample pyrolysed at 1050 °C versus Li/Li$^+$ in comparison with pure graphite/Li even if the graphite content is 25 wt% lower.

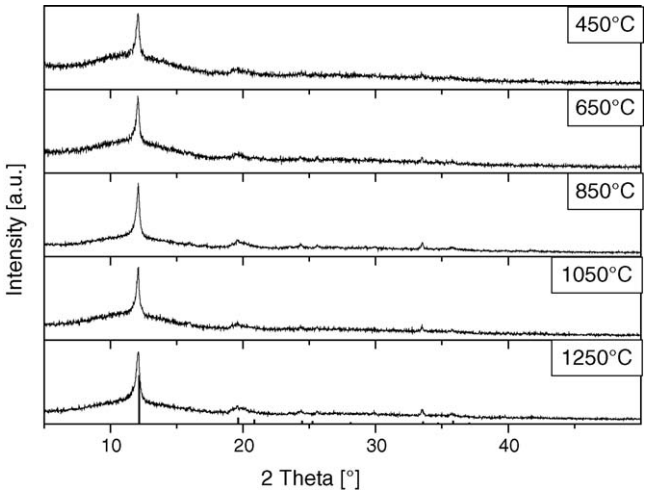

Fig. 3. X-ray diffraction patterns of 25VL20-75C pyrolysed at different temperatures; graphite phase is marked with bars.

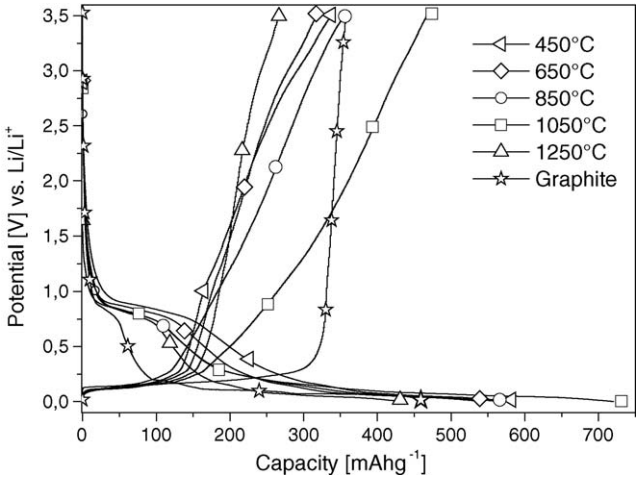

Fig. 4. First charge- and discharge of 25VL20-75C samples pyrolysed at different temperatures compared to pure graphite vs. Li/Li$^+$.

The coulombic efficiency (η) increases with higher pyrolysis temperatures leading to a maximum of 64.8% at 1050 °C and decreases at higher temperatures (see Table 2). The η-value is 12.2% lower than the coulombic efficiency of pure graphite powder analysed here.

Table 2
Capacity of the first charge (C_{charge}) and discharge ($C_{discharge}$) cycle vs. Li/Li$^+$, coulombic efficiency (η), nitrogen and oxygen content and specific surface area (S_A) of 25VL20-75C powder samples pyrolysed at different temperatures in comparison to commercial graphite

T_{pyr} (°C)	C_{charge} (mA hg^{-1})	$C_{discharge}$ (mA hg^{-1})	η (%)	N (wt%)	O (wt%)	S_A (m^2/g)
450	582	337	57.9	3	5.9	220
650	539	317	58.8	3.1	7.2	170
850	566	356	62.9	3.3	9.2	65
1050	731	474	64.8	2.1	11.3	124
1250	431	266	61.7	3.5	5.6	64
Graphite	459	357	77	–	0.09	14

Since optimized graphite anodes exhibit an efficiency of nearly 100%, the effort of our investigation is to suppress the loss of capacity. The reason for the loss of capacity is discussed as follows:

Generally, the irreversible capacity, which is defined as the loss of capacity after two consecutive charge and discharge cycles, is based on two effects, namely the incorporation of solvated lithium and the formation of a solid electrolyte interphase (SEI). The former one resembles in a plateau at potentials between 0.8 to 0.2 V versus Li/Li^+ and mainly proceeds at the prismatic surface of the graphite particles. The formation of a SEI, therefore, occurs at potentials exceeding 0.8 V versus Li/Li^+.[27] These phenomena are mainly affected by the particle size, the morphology and the surface area of the used graphite.

Zaghib et al.[28] analysed graphite with different particle sizes and found a correlation between BET surface area and irreversible capacity. They found that the main factor is not only given by the BET surface area but by the amount of edge plane sites present at a certain surface area. Yoshio et al. discovered an enhanced reversible capacity if graphite particles are milled to spheres coated with carbon by thermal vapour deposition (TVD).[29] They attributed the improvement by a non-orientation of the graphite particles caused by the milling process and containing mainly basal surface planes by the TVD coating. Béguin et al.[30] also improved the electrochemical properties by CVD coating on graphite. They explained the gain of coulombic efficiency to a reduced active surface area (ASA), which is related to BET, additionally, taking the active surface sites into account. Winter et al. reported on a correlation between the BET surface, particle size and the irreversible capacity. They presented a model where thick graphite flakes undergo less solvated intercalation than thinner ones having the same particle size distribution.[31] This effect is explained by the larger amount of solvated lithium that can be incorporated in thinner particles in the prismatic planes. Due to the strain on the internal gaps in thicker particles, solvated intercalation can only take place in the outer gaps.

Fig. 5a and b show SEM images of pure graphite compared with our SiCN/graphite composite powder. The change of morphology due to the additional SiCN phase is obvious. The SiCN phase seems to cover the graphite particles leading to a cauliflower-like structure exemplarily shown for the sample pyrolysed at 1050 °C in Fig. 5a. The morphology change leads to a higher specific surface area (Table 2) and thus to a larger irreversible capacity due to an enlarged SEI layer formed. Consequently the beginning of the plateau at 0.8 V is shifted to higher capacities (Fig. 4). Main fraction of the irreversible capacity in this case is given by the incorporation of solvated lithium reflected by the enhanced plateau at 0.8 V. This finding implies that the SiCN phase not only incorporates lithium reversibly but also incorporates a large amount of solvated lithium within the first cycle. With higher pyrolysis temperature the SiCN particles accrete and the specific surface area decreases. Hence, the amount of SEI as well as the amount of solvated lithium intercalation decrease, which leads to higher coulombic efficiency (Table 2). Pure graphite, therefore, exhibits mainly basal surface planes as can be seen in the SEM image (Fig. 5b) making it reasonable that a lower amount of solvated lithium is incorporated and the plateau at 0.8 V is less pronounced. As these correlations are only valid for pyrolysis temperatures up to 1050 °C an additional effect has to be considered to explain the drop of capacity and efficiency at pyrolysis temperatures of 1150 °C. In Table 2 it is shown that the oxygen concentration in SiCN increases up to 1050 °C and decreases at higher pyrolysis temperatures. Above 1100 °C the reaction of oxygen with carbon or silicon forms evaporable SiO and CO, which subsequently reduces the oxygen content in the SiCN phase. It can be also seen from Table 2 that a higher amount of oxygen is correlated with higher reversible capacities and higher coulombic efficiencies. This result emphasizes a major role of oxygen in this system, which was also reported for pure graphite.[32] The oxygen content in our samples is probably attributed to the milling time. Increasing milling time resulted in increasing oxygen content.

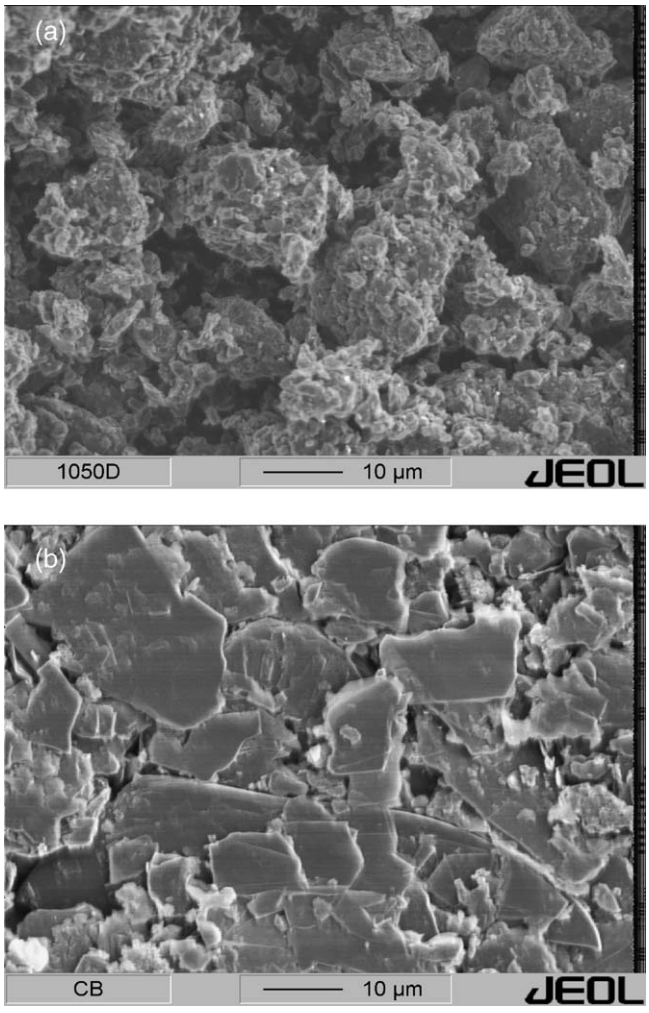

Fig. 5. (a) SEM image of 25VL20-75C powder sample pyrolysed at 1050 °C. (b) SEM image of pure graphite powder.

The cycling performance of 25VL20-75C pyrolysed at 1050 °C, shown in Fig. 6, exhibits remarkable features, since the specific charge increases with increasing cycle numbers.

The interpretation of this phenomenon is not clear yet but due to solvated lithium incorporated in the SiCN phase one could assume that this reaction is not fully irreversible. In con-

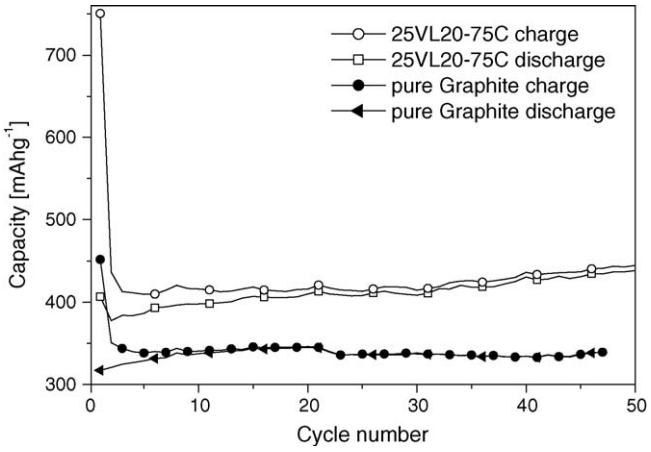

Fig. 6. Change of capacity after the first 50 cycles of 25VL20-75C powder sample pyrolysed at 1050 °C compared to pure graphite powder vs. Li/Li^+.

trast, the capacity of the particular graphite used here slightly decreases with the number of cycles due to exfoliation. It should be mentioned here that we used a commercial graphite powder not optimized for electrochemical applications. However, it is clear from our work that amorphous SiCN is an active phase that influences the intercalation mechanism and indicates protection of graphite from exfoliation. Especially the chemical stability of the SiCN phase in combination with different electrode and electrolyte systems is of high interest for further developing alternative materials suitable for Li-ion batteries.

4. Conclusion and outlook

For the first time the electrochemical properties of a graphite/polymer derived SiCN composite were analysed with respect to its application as anode material in secondary lithium ion batteries. A reversible capacity of 474 mA hg^{-1} was attained, which is 1.3 times higher compared with the value of 357 mA hg^{-1} analysed for commercial graphite powder versus Li/Li^+. This finding indicates that the SiCN phase is an active phase in terms of lithium intercalation/deintercalation and that it is a promising candidate as protective layer on graphite, due to its chemical stability. Still unfavourable is the low coulombic efficiency due to the large specific surface area of the formed SiCN phase. Therefore, future work will be focused on reducing the surface area to improve the electrochemical properties. Furthermore, the influence of the amorphous SiCN layer on the capacity and chemical stability of other electrode materials like silicon and optimized carbon materials as well as on different electrolytes is of particular interest.

Acknowledgement

We gratefully acknowledge the financial support by the Deutsche Forschungsgemeinschaft (DFG), Bonn, Germany (SFB 595/A4).

References

1. Megahed, S. and Scrosati, B., Lithium-ion rechargeable batteries. *J. Power Sources*, 1994, **51**, 79–104.
2. Megahed, S. and Ebner, W., Lithium-ion battery for electronic applications. *J. Power Sources*, 1995, **54**, 155–162.
3. Nazri, G.-A. and Pistoia, G., *Lithium Batteries, Science and Technology*. Kluwer Academic Publishers, 2004.
4. Jacobson, A. J., Chianelli, R. R. and Whittingham, M. S., Amorphous Molybdenum disulfide Cathodes. *J. Electrochem. Soc.*, 1979, **126**(12), 2277–2278.
5. Besenhard, J. O., Gürtler, J., Komenda, P. and Josowicz, M., Suppression of dendrite formation during cycling of lithium electrodes in organic electrolytes. *Proc. Electrochem. Soc.*, 1988, **88**(6), 618–626.
6. Kanno, R., Takeda, Y., Ichikawa, T., Nakanishi, K. and Yamamoto, O., Carbon as negative electrodes in lithium secondary cells. *J. Power Sources*, 1989, **26**(3–4), 535–543.
7. Mohri, M., Yanagisawa, N., Tajiama, Y., Tanaka, H., Mitate, T., Nakajiama, S. *et al.*, Rechargeable lithium battery based on pyrolytic carbon as a negative electrode. *J. Power Sources*, 1989, **26**(3–4), 545–551.
8. Nagaura, T. and Tozawa, K., Lithium ion rechargeable battery. *Prog. Batteries Sol. cells*, 1990, **9**, 209–217.
9. Besenhard, J. O., Yang, J. and Winter, M., Will advanced lithium-alloy anodes have a chance in lithium-ion batteries? *J. Power Sources*, 1997, **68**(1), 87–90.
10. Scrosati, B., Recent advances in lithium ion battery materials. *Electrochem. Acta*, 2000, **45**, 2461–2466.
11. Li, H., Wang, Q., Shi, L., Chen, L. Q. and Huang, X. J., Nano-alloy anode for lithium ion batteries. *Solid State Ionics*, 2002, **148**(3–4), 247–258.
12. Bourderau, S., Brousse, T. and Schleich, D. M., Amorphous silicon as a possible anode material for Li-ion batteries. *J. Power Sources*, 1999, **82**, 233–236.
13. Jung, H. J., Park, M., Yoon, Y. G., Kim, G. B. and Joo, S. K., Amorphous silicon anode for lithium-ion rechargeable batteries. *J. Power Sources*, 2003, **115**(2), 346–351.
14. Yoshio, M., Wang, H., Fukuda, K., Umeno, T., Dimov, N. and Ogumi, Z., Carbon-coated Si as a lithium-ion battery anode material. *J. Electrochem. Soc.*, 2002, **149**(12), A1598–A1603.
15. Hatchard, T. D. and Dahn, J. R., In Situ XRD and Electrochemical Study of the Reaction of Lithium with Amorphous Silicon. *J. Electrochem. Soc.*, 2004, **151**(6), A383–A842.
16. Wu, Y. P., Jiang, C. Y., Wan, C. R., Fang, S. B. and Jiang, Y. Y., Nitrogen-containing polymeric carbon as anode material for lithium ion secondary battery. *J. Appl. Polym. Sci.*, 2000, **77**, 1735–1741.
17. Wu, Y. P., Li, Y. X., Fang, S. B. and Jiang, Y. Y., Carbon anode materials based on copolymers of nitrogen-containing monomers with DVB. *J. Mater. Sci.*, 1999, **34**, 4253–4258.
18. Wu, Y. P., Fang, S. B. and Jiang, Y. Y., Carbon anode materials based on melamine resin. *J. Mater. Chem.*, 1998, **8**(10), 2223–2227.
19. Zhang, X. W., Patil, P. K., Wang, C. S., Appleby, A. J., Little, F. E. and Cocke, D. L., Electrochemical performance of lithium ion battery, nano-silicon-based, disordered carbon composite anodes with different microstructures. *J. Power Sources*, 2004, **125**(2), 206–213.
20. Liu, Y., Hanai, K., Yang, J., Imanishi, N., Hirano, A. and Takeda, Y., Morphology-stable silicon-based composite for Li-intercalation. *Solid State Ionics*, 2004, **168**(1–2), 61–68.
21. Yoshio, M., Wang, H. and Fukuda, K., Sperical carbon-coated natural graphite as a lithium-ion battery anode material. *Angew. Chem.*, 2003, **42**(35), 4203–4206.
22. Holzapfel, M., Buqa, H., Krumeich, F., Novak, P., Petrat, F.-M. and Veit, C., Chemical vapor deposited silicon/graphite compound material as negative electrode for lithium-ion batteries. *Electrochem. Solid-State Lett.*, 2005, **8**(10), A516–A520.
23. Gregori, G., Kleebe, H.-J., Brequel, H., Enzo, S. and Ziegler, G., Microstructure evolution of precursors-derived SiCN ceramics upon thermal treatment between 1000 and 1400°C. *J. Non-Cryst. Solids*, 2005, **351**, 1393–1402.
24. Li, L.-Y., Kroke, E., Riedel, R., Fasel, C., Gervais, C. and Babonneau, F., Thermal cross-linking and pyrolytic conversion of

poly(ureamethylvinyl)silazanes to silicon-based ceramics. *Appl. Organomet. Chem.*, 2001, **15**, 820–832.
25. Buiel, E., George, A. E. and Dahn, J. R., On the reduction of lithium insertion capacity in hard-carbon anode materials with increasing heat-treatment temperature. *J. Electrochem. Soc.*, 1998, **145**(7), 2252–2257.
26. Larcher, D., Mudalige, C., George, A. E., Porter, V., Ghaghouri, M. and Dahn, J. R., Si-containing disordered carbons prepared by pyrolysis of pitch/polysilane blends: effect of oxygen and sulphur. *Solid State Ionics*, 1999, **122**, 71–83.
27. Fong, R., von Sacken, U. and Dahn, J. R., Studies of lithium intercalation into carbons using nonaqueous electrochemical cells. *J. Electrochem. Soc.*, 1990, **137**(7), 2009–2013.
28. Zaghib, K., Nadeau, G. and Kinoshita, K., Effect of graphite particle size on irreversible capacity loss. *J. Electrochem. Soc.*, 2000, **147**(6), 2110–2115.
29. Yoshio, M., Wang, H., Fukuda, K., Umeno, T., Abe, T. and Ogumi, Z., Improvement of natural graphite as a lithium-ion battery anode material, from raw flake to carbon-coated sphere. *J. Mater. Chem.*, 2004, **14**, 1754–1758.
30. Béguin, F., Chevallier, F., Vix, C., Saadallah, S., Rouzaud, J. N. and Frackowiak, E., A better understanding of the irreversible lithium insertion mechanisms in disordered carbons. *J. Phys. Chem. Solids*, 2004, **65**, 211–217.
31. Winter, M., Novak, P. and Monnier, A., Graphites for lithium-ion cells: the correlation of the first-cycle charge loss with the brunauer-emmett-teller surface area. *J. Electrochem. Soc.*, 1998, **145**(2), 428–436.
32. Hung, C.-C. and Clark, G. W., Effects of surface oxygen on the performance of carbon as an anode in lithium-ion batteries. *Proc. Electrochem. Soc.*, 2001, **2000–21**, 172–192.